

# SHEAR FLOW IN A MILDLY SLOPING RIFFLE-POOL SEQUENCE

**Bruce MacVicar, Lana Obach**

Department of Civil and Environmental Engineering  
University of Waterloo  
200 University Avenue W, Waterloo, ON Canada N2G 3L1  
[bmacvicar@uwaterloo.ca](mailto:bmacvicar@uwaterloo.ca), [lobach@uwaterloo.ca](mailto:lobach@uwaterloo.ca)

**Sibel Kara, Thorsten Stoesser**

School of Civil and Environmental Engineering  
Georgia Institute of Technology  
Mason Building, 790 Atlantic Drive, Atlanta, GA 30332-0355  
[sibel.kara@ce.gatech.edu](mailto:sibel.kara@ce.gatech.edu), [thorsten@ce.gatech.edu](mailto:thorsten@ce.gatech.edu),

**Jim Best**

Depts of Geology, Geography, Mech. Science and Eng., and Ven Te Chow Hydrostems Laboratory  
University of Illinois at Urbana-Champaign  
Natural History Building, 1301 West Green Street, Urbana, IL, 61801-2938  
[jimbest@illinois.edu](mailto:jimbest@illinois.edu)

## ABSTRACT

A series of physical experiments, together with Large Eddy Simulations (LES), are performed for an open channel flow over a mildly sloping pool-riffle sequence, a bed morphology typical in many coarse-grained rivers. Five low-angled ( $7.2^\circ$ ) bedforms were placed in a 0.6m wide rectangular flume with a flow Reynolds number of approximately  $Re=20,000$ . Our broad goal is to develop a general model of flow over this simplified macroscale bedform. Specific objectives were to measure changes to the three-dimensional distribution of flow and describe turbulent shear zones that form due to pressure gradients and interactions with the side wall. A new parameter,  $\Psi$ , is introduced to describe the lateral distribution of flow. Flow over the bedforms is characterized by a three-dimensional redistribution of flow and increased generation of turbulence in zones of flow deceleration, particularly near the side walls of the channel. Over repeated bedforms, the distribution of flow and turbulence adjust towards a type of equilibrium characterized by stronger lateral gradients in velocity and Reynolds stress.

## INTRODUCTION

Riffle-pool sequences are a common feature of open channels. They are characterized by a vertical undulation of the bed and are typically associated with planform sinuosity in natural rivers, such that deep pools occur in bends and shallow riffles occur in the intervening straight channel sections. Pool-riffle sequences are distinct from dunes and other bedforms

because they are mildly sloping, which means that flow separation does not occur at the crest, and they exhibit a consistent scaling relation with channel width. Despite past extensive theoretical analysis and comprehensive field campaigns to investigate flow and sediment dynamics, no adequate understanding exists to explain the scaling relation between channel width and bedform spacing, although we know that the feedback between flow and sediment transport seems to promote accumulation of sediment that grows to become dominant features of the channel.

At the root of the problem is an inadequate understanding of how macrobedforms, such as riffle-pool sequences, alter the distribution of flow and turbulence. Early field tests suggested that the magnitude of near-bed velocity vectors increased more rapidly in deep pools than in other areas of the channel, but no physical justification was found for this observation (Keller, 1971), and subsequent attempts at verification were inconclusive (Clifford, 1992). Field and flume experiments have cited increased turbulence (Hassan and Woodsmith, 2004) and lateral convergence of flows (MacWilliams et al., 2006) as critical phenomena, but it is not clear how to reconcile seemingly divergent theories. In a straight artificial pool, MacVicar and Rennie (in review) argued that the phenomena are linked aspects of convective acceleration and deceleration, and that they may all be significant for pool scour.

The experiments described herein are part of a program of physical and numerical experiments to develop a general model of the hydrodynamics of macrobedforms. The objectives of this article are to: i) measure the degree to which

macrobedforms redistribute flow over a series of mildly sloping pools and riffles and ii) clarify the nature of turbulence generated in shear zones over these macrobedforms.

## METHODOLOGY

### Flume experiments

The experimental facility is a 17 m long 0.6 m wide flume located at the Ven Te Chow Hydrosystems Laboratory, University of Illinois at Urbana-Champaign. Bedforms were constructed from PVC sheets in a modular arrangement so that different channel and bedform geometries could be tested. In this article, we describe an experiment in which five bedforms were placed in series. Each bedform was 1.82 m long and was comprised of a transition section, angled at  $7.2^\circ$  above the horizontal, followed by a flat section of shallow flow, a transition section at  $7.2^\circ$  below the horizontal, and a flat section of uniform flow (Figure 1). The gradual angle of the transitions ensured that permanent flow separation did not occur. Flow velocities were measured in the first and fourth pools of the bedform series.

An array of 4 MHz Ultrasonic Doppler Velocity Profilers (UDVPs; see Best et al., 2001 for details of UDVP) was used to measure flow velocities. UDVPs measure velocities at high frequencies in a series of bins along the beam axis. The recorded velocity vectors measure the component of flow in the orientation of the beam. UDVP parameters were set to record signals at 25 Hz in bins that were 1 to 2 mm long in the beam direction and 5 to 6 mm in diameter. Depending on channel depth, between 50 and 100 bins were defined along the beam axis. Four to twelve profiles were measured across one half of the channel width, and cross-sections were spaced between 0.4 and 1.0 m in the streamwise direction, with closer sections over bedforms and wider spacing in longer uniform sections.

Orthogonal velocity and Reynolds stress were calculated in the sampling volume on a three-dimensional orthogonal grid. These variables were calculated from beam velocities that were recorded at orientations of  $30^\circ$ ,  $0^\circ$  and  $-30^\circ$  to the vertical ( $u_1$ ,  $u_2$ , and  $u_3$  respectively) following Pedocchi and Garcia (2009). Streamwise ( $u$ ) and vertical velocities ( $w$ ) are calculated as:

$$u = \frac{\overline{u_1 - u_3}}{2 \sin \alpha}$$

$$w = -\frac{\overline{u_1 + u_3}}{2 \cos \alpha} = -\overline{u_2}$$

and the principal Reynolds stress ( $-u'w'$ ) is:

$$-u'w' = -\frac{\overline{u_1'^2 + u_3'^2}}{2 \sin^2 \alpha}$$

To obtain beam velocities at grid node locations, measurements of  $u_1$ ,  $u_2$ , and  $u_3$  were interpolated through the sampling volume prior to the calculation of the orthogonal components and the principal Reynolds stress.

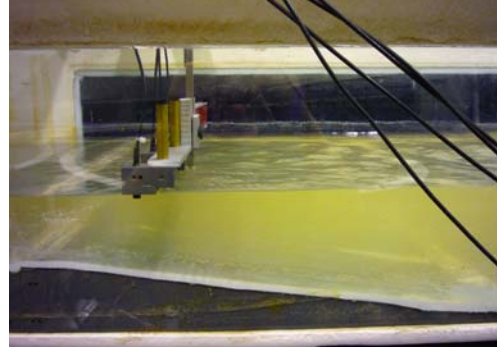


Figure 1. A mildly sloping pool-riffle form in the experimental flume. The channel is 0.6 m wide and the bedforms are 0.06m high. An array of Ultrasonic Doppler Velocity Profilers is also shown.

### Analysis of flow distribution

Flow distribution parameters were calculated to quantify changes to the distribution of flow as a result of the bedforms. Following the Clauser method, the shear velocity ( $u^*$ ) was calculated by fitting the log law to velocity-elevation pairs within the inner zone:

$$\frac{u}{u^*} = \frac{1}{\kappa} \ln \left( \frac{zu^*}{\nu} \right) + A$$

where  $\nu$  is the kinematic viscosity,  $\kappa$  is von Karman's constant ( $\sim 0.4$ ) and  $A$  is a constant of integration ( $\sim 5.0$ ). Following Coles (1956) and Kironoto and Graf (1995), the wake parameter ( $\Pi$ ) was calculated by fitting velocity-elevation pairs over the entire flow depth to the velocity defect law:

$$\frac{u_{\max} - u}{u^*} = -\frac{1}{\kappa} \ln \left( \frac{z}{z_{u \max}} \right) + \frac{2\Pi}{\kappa} \sin^2 \left( \frac{\pi}{2} \frac{z}{z_{u \max}} \right)$$

To describe the lateral distribution of flow, a new lateral convergence parameter was defined as

$$\Psi = \frac{U}{U_b}$$

where  $U$  is the depth-averaged velocity and  $U_b$  is the bulk or section-averaged velocity.  $\Psi$  will increase in a downstream direction due to flow convergence and decrease due to flow divergence.

### Numerical modelling

Large Eddy Simulations (LES) were performed with the code HYDRO3D-GT. This is a successor of the code HYDRO3D originally developed at the University of Bristol (Stoesser, 2002). The code solves the filtered incompressible Navier-Stokes equations on block-structured curvilinear grids using a cell-centered Finite-Volume method with collocated storage of the Cartesian velocity components. Second-order central differences are employed for the convective as well as for the diffusive terms. A fractional-step method is used with a Runge-Kutta predictor and the solution of a pressure-correction equation in the final step as a corrector. The code is parallelized and domain decomposition is used to speed up the

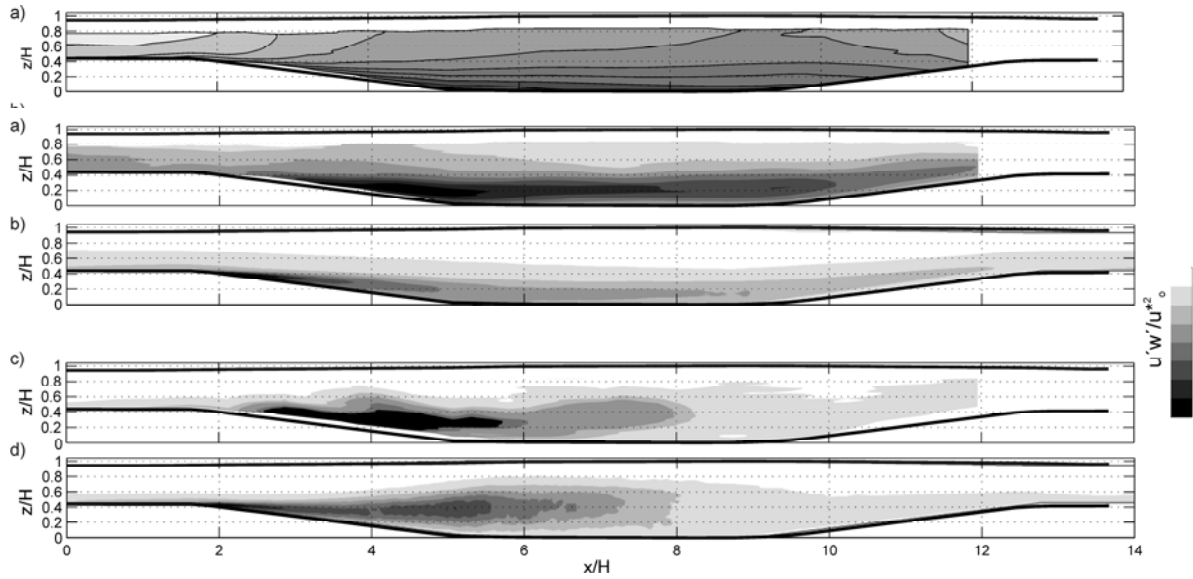


Figure 3. Comparison of Reynolds stress ( $u'w'$ ) distribution at centerline for experimental (a) and LES simulation (b) and at 10% of the channel width for experimental (c) and LES simulation (d). Reynolds stress is normalized by the square of the shear velocity at  $x/H = 0$  ( $u_*^2$ ). Flow direction is from left to right.

simulation.

The LES domain covered one full pool-riffle sequence in the longitudinal direction and the full width of the flume in the spanwise direction. A geometrically periodic system was created numerically by using cyclic boundary conditions in the flow direction. For the smooth bed and the side-walls, the no-slip wall boundary condition was employed, with three grid points within the viscous sublayer. The free surface was approximated with a rigid lid at which a slip condition was used.

## RESULTS

### Comparison between Experimental and LES Results

The velocity distribution in the channel as measured in the fourth pool of the series and from LES simulations is characterized by streamwise acceleration and deceleration as a result of the depth changes over the bedform (Figure 2). Due to the small change in slope of the bed, there is no region of permanent flow separation and the streamwise velocity decelerates markedly on the down-slope into the pool. The flow deceleration is more pronounced near the sidewall

(Figure 2c,d), and there is a large area of low momentum flow near the bed at the entrance to the pool. This is a result of the presence of the side wall and the comparably weak secondary currents, relative to the uniform sections, on the down-slope. As flow depth decreases in the pool, the near-bed velocities increase such that the vertical gradient in velocity from the bed to the water surface is reduced. These results are common to the LES simulations and measurements in both the first and fourth pools and are in broad agreement with what is expected in decelerating and accelerating flows (Kironoto and Graf, 1995).

A substantial difference in the distribution of streamwise velocity between the experimental and LES results was found at the channel centerline. While the experimental results show a positive relation between velocity and height throughout the pool, LES simulations indicated that a velocity dip (i.e. a velocity peak below the water surface) is expected in this area. The reason for this discrepancy is thought to be related to a rigid lid assumption for the simulations. Secondary flow vectors appear to be stronger in the numerical simulations and are forcing this perceived dip in velocities.

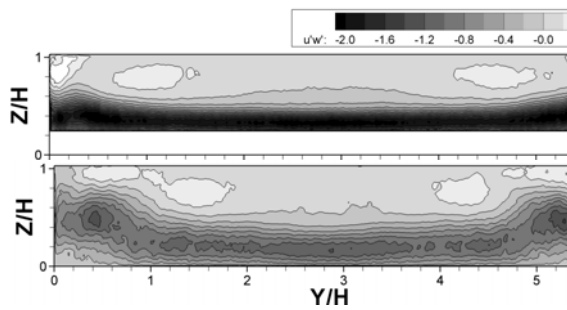


Figure 4. Distribution of the normalized turbulent shear stress in two selected cross-sections from LES simulations: halfway on the down-slope (upper part) and in the middle of the pool (lower part).

The distribution of Reynolds stress (Figure 3) is dominated by a high stress zone that forms downstream of the crest of the bedform in a zone of flow deceleration, and is likely due to a shear layer formed in this region of expanding flow. For both the experimental results and the LES simulations, the highest shear stresses are found at the beginning of the down-slope and reach values approximately three-times the global wall shear stress. Measured experimental Reynolds stresses were typically higher than estimates based on LES simulations. Possible explanations for this discrepancy include additional unmeasured roughness in the experimental facility and because only the resolved Reynolds stresses are plotted for the LES results. Both experimental and numerical simulations show that Reynolds stress increases and then decreases in the deep part of the pool.

The zone of high stress first appears near the bed but moves higher in the water column in the middle of the pool as the magnitude of stresses decreases.

In the cross-section of the down-slope (Figure 4), the highest Reynolds stresses are found in the corners near the bed, which is where most of the fluid shear takes place. The secondary currents in the shallow part of the channel transport high momentum fluid towards the corners (not shown), and as the flow enters the down-slope this high momentum fluid coincides with low-momentum corner fluid and results in the aforementioned shear layer. This shear layer is tilted towards the water surface, which is why areas with maximum Reynolds stresses are found away from the bed. On the down-slope, pockets of high turbulent shear stress are found in the channel corners, while further downstream in the middle of the pool the turbulent shear stress peaks occur away from the bed.

To aid simultaneous visualization of flow distribution and Reynolds stress within the experimental sampling volumes, a three-dimensional plot of velocity vectors and locations of high Reynolds stress was developed (Figure 5). Only the deep uniform sections are shown in each case to improve readability. Key observations are that turbulence and velocity gradients are high in the pools. High Reynolds stresses occur across the entire width and continue through Pool 1. In contrast, lateral velocity gradients are stronger in Pool 4 and the zone of high Reynolds stress is much smaller. Results from Pool 4 match more closely with the LES simulations, which use cyclic boundary conditions in the streamwise direction.

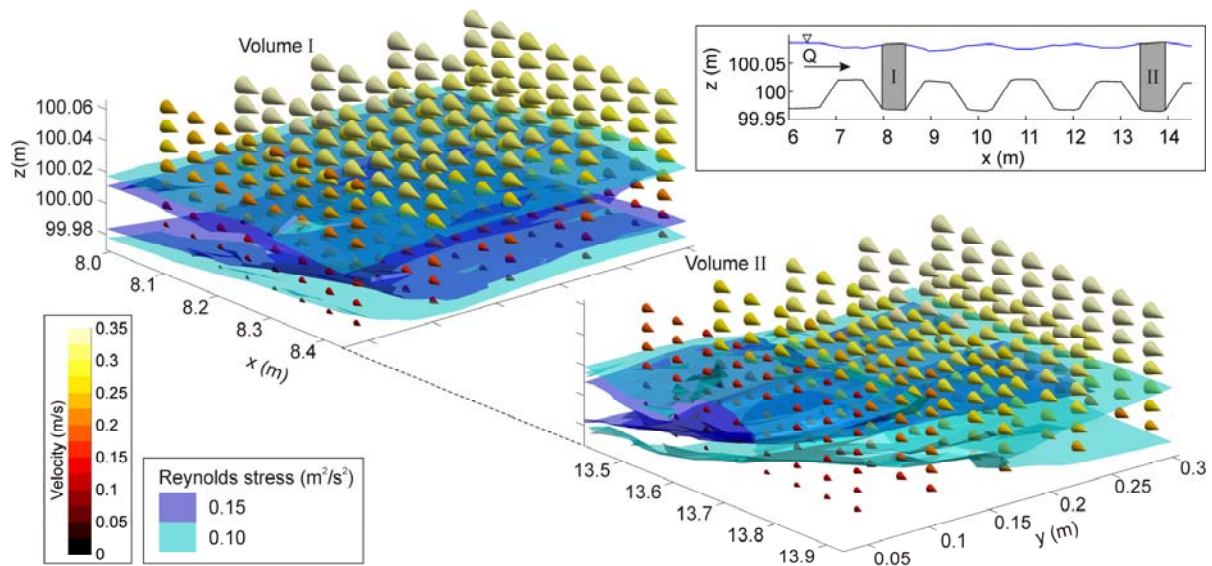


Figure 5. Coneplot of velocity vectors overlain with contour surfaces of Reynolds stress. The size and color of cones represent the velocity magnitude, while the direction of the cones corresponds with the direction of three dimensional fluid flow. Volume I is the first pool in the sequence and Volume II is the fourth pool in the sequence, as shown in the inset figure. The channel centerline is at  $y = 0.3$  m, meaning that one half of the channel is represented with the side wall at  $y = 0$ .

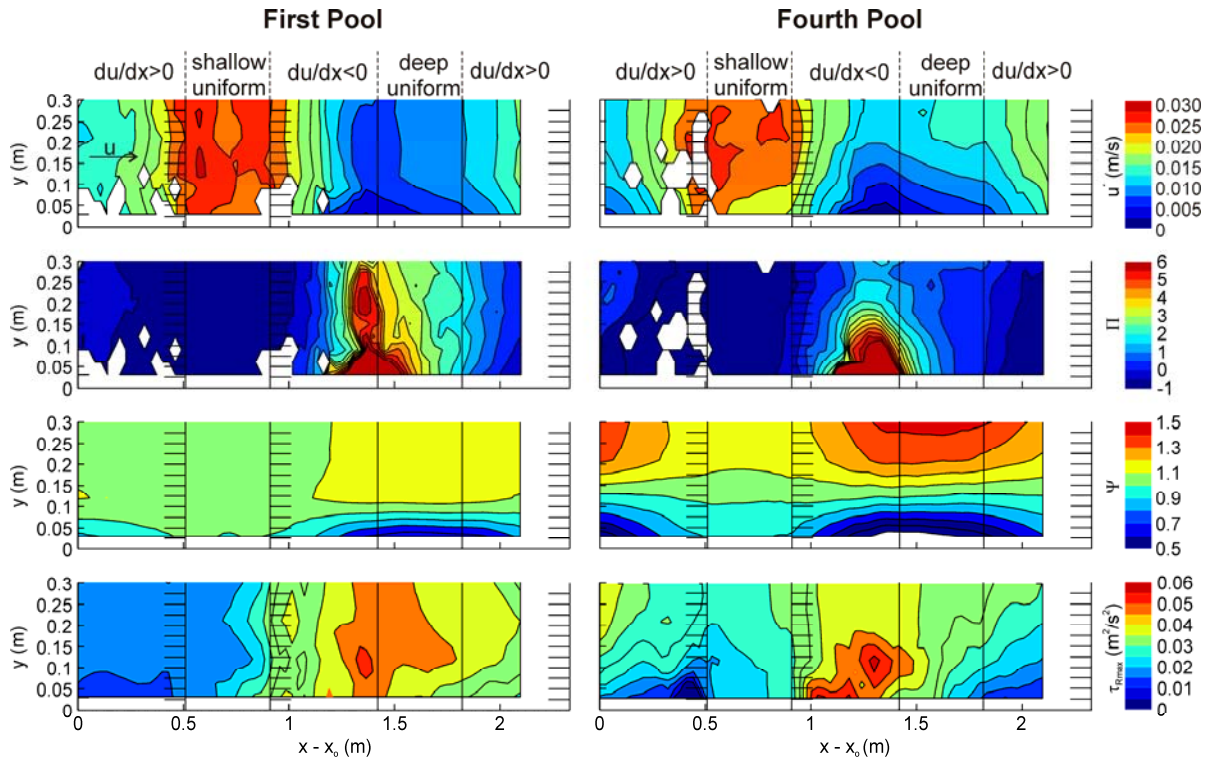


Figure 6. Planform distribution of variables that describe the velocity distribution including the shear stress ( $\tau_u$  – calculated from slope of inner zone), Coles wake parameter ( $\Pi$  – shape parameter fit to mean velocity in outer zone), and the lateral flow distribution parameter ( $\Psi$ ). The maximum Reynolds stress in the profile ( $\tau_{Rmax}$ ) is also shown.

### Flow distribution parameters

The influence of these macrobedforms on flow distribution is more easily demonstrated by calculating flow distribution parameters to describe the inner zone ( $u^*$ ), the outer zone ( $\Pi$ ) and the lateral distribution ( $\Psi$ ) (Figure 6). In the first pool of the bedform series, the deep flow area is characterized by lower shear velocities, positive values of  $\Pi$ , which indicates higher momentum in the outer flow zone, and higher values of  $\Psi$ , which indicates that flow is converging laterally towards the center of the channel in the pool. The changes to flow distribution within the pool are accompanied by high Reynolds stress, with a peak value near to the side wall at a location coincident with low shear velocities, maximum  $\Pi$  values, and a strong lateral gradient in  $\Psi$ , confirming the presence of a lateral shear zone.

By the fourth pool, the lateral gradients in the flow distribution parameters are increased such that a band of higher shear velocity occurs through the center of the pool, peak values in  $\Pi$  are restricted to near the side-wall, and the lateral convergence and divergence of flow in the deep pool and the shallow riffle is more pronounced. Peaks in Reynolds stress in the fourth pool are concentrated in the side-wall area.

By isolating the channel centerline, it is clear that the initial hydrodynamic response to the bedforms differs from that to a sequence of bedforms (Figure 7). The shear velocity  $u^*$ , for instance, is higher through the pool and downstream in

the fourth pool than in the first. The wake parameter  $\Pi$  shows that there is a decreased variability in the vertical distribution of flow as  $\Pi$  is generally closer to zero, which occurs for uniform flow distributions, in the fourth pool than in the first. In contrast, with more uniform vertical flow distributions,  $\Psi$  is always higher in the fourth pool, with minimum values of about  $\Psi = 1.5$  approximately equal to the maximum value in the first pool. This indicates that there is a progressive increase in the lateral concentration of flow through the series of bedforms.

The distribution of flow appears to be close to a stable pattern in the fourth pool. By examining the values for  $u^*$ ,  $\Pi$  and  $\Psi$  at the beginning of the two sections where  $du/dx > 0$ , it is apparent that the differences between the upstream and downstream values of these parameters are much smaller in the fourth pool than the first. This upstream and downstream similarity suggests that the patterns observed in the fourth pool are similar to what would be observed in a longer series of bedforms or in numerical simulations that use periodic boundary conditions.

### CONCLUSIONS

The work presented herein is significant because of the improved description of flows in non-uniform channels and in the identification of phenomena that are likely to be

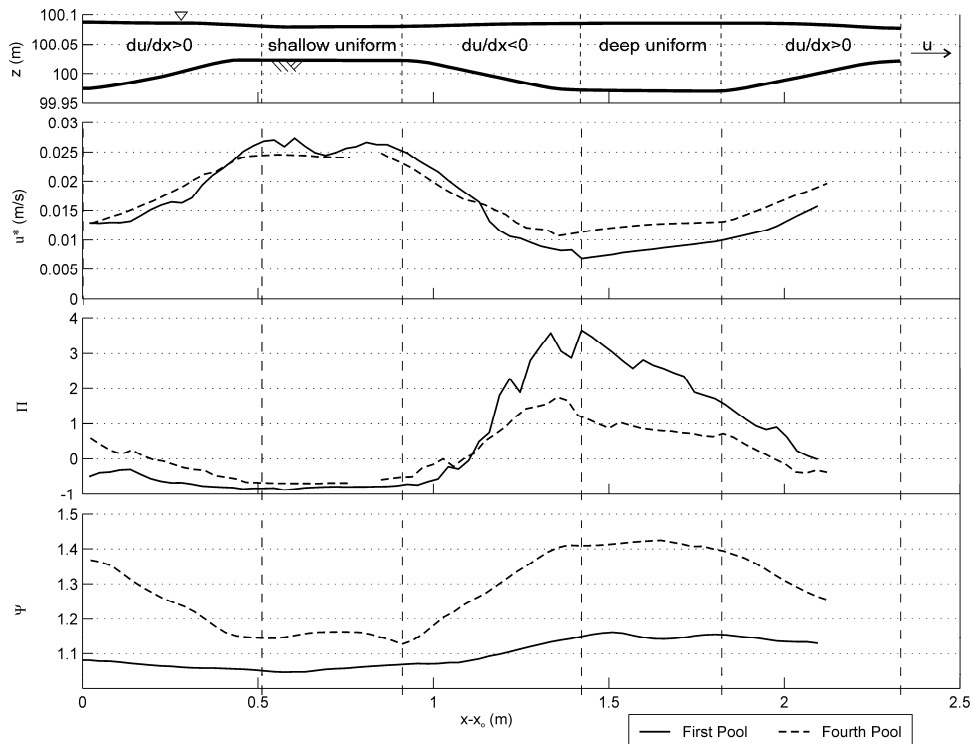


Figure 7. Centerline values of variables that describe the velocity distribution including the shear stress ( $\tau_u$  – calculated from slope of inner zone), Coles wake parameter ( $\Pi$  – shape parameter fit to mean velocity in outer zone), and the lateral flow distribution parameter ( $\Psi$ ).

significant for understanding flow through open channels with large-scale bedforms. Specific conclusions are:

- 1) The description of flow distribution was improved by the introduction of a new parameter  $\Psi$  to describe the lateral distribution of flow.
- 2) Flow over low-angled bedforms is characterized by a three-dimensional redistribution of flow and increased generation of turbulence in zones of flow deceleration, particularly near the side walls of the channel.
- 3) The uniform flow sections in the tested bedform geometry were not sufficiently long to allow the recovery of a uniform flow distribution.
- 4) Over repeated bedforms, the distribution of flow appears to adjust towards a type of equilibrium with stronger lateral gradients in velocity and Reynolds stress.

## REFERENCES

- Best, J.L., A.D. Kirkbride, and J. Peakall, 2001, "Mean flow and turbulence structure of sediment-laden gravity currents: new insights using ultrasonic Doppler velocity profiling". In: *Particulate Gravity Currents* (Eds W.D. McCaffrey, B.C. Kneller and J. Peakall), *IAS Special Publications*, 31, pp 159–172.
- Clifford, N. J. and K. S. Richards, 1992, "The reversal hypothesis and the maintenance of riffle-pool sequences: a

review and field appraisal", *Lowland Floodplain Rivers: Geomorphological Perspectives*, P. Carling and G. E. Petts, eds., Chichester, UK, Wiley, pp. 43-70.

Coles, D., 1956, "The law of the wake in the turbulent boundary layer", *Journal of Fluid Mechanics*, Vol. 1, pp. 191-226.

Keller, E. A., 1971, "Areal sorting of bed material: the hypothesis of velocity reversal", *Geological Society of America Bulletin*, Vol. 82, pp. 753-756.

Kironoto, B. A. and W. H. Graf, 1995, "Turbulence characteristics in rough non-uniform open-channel flow", *Proceedings of the Institution of Civil Engineers-Water Maritime and Energy*, Vol. 112, pp. 336-348.

MacWilliams, M. L. J., J. M. Wheaton, et al., 2006. "Flow convergence routing hypothesis for pool-riffle maintenance in alluvial rivers", *Water Resources Research*, Vol. 42, W10427.

MacVicar, B. J. and C. D. Rennie, in review. "Secondary currents, shear stress and turbulence in a straight artificial pool", *Water Resources Research*.

Pedocchi, F. and M. H. Garcia, 2009. "Application of an Ultrasonic Velocity Profiler for velocity and suspended sediment measurements in an oscillatory boundary layer", *Civil Engineering Studies: Hydraulic Engineering Series*, Urbana, Illinois, University of Illinois, Report 83, 53 pgs.

Stoesser, T., 2002, *Development of Validation of a CFD Code for Turbulent Open-Channel Flows*, PhD thesis, University of Bristol, UK.